Colloids and Surfaces B: Biointerfaces 231 (2023) 113577

Contents lists available at ScienceDirect

Colloids and Surfaces B: Biointerfaces

journal homepage: www.elsevier.com/locate/colsurfb

Optimization of the immunorecognition layer towards *Brucella sp.* on gold surface for SPR platform

Laura Pasquardini [a,*], Lia Vanzetti [b], Roberto Canteri [b], Nunzio Cennamo [c], Francesco Arcadio [c], Chiara Perri [d], Girolamo D'Agostino [d], Rosalba Pitruzzella [c], Riccardo Rovida [c], Alessandro Chiodi [d], Luigi Zeni [c,*]

[a] *Indivenire srl, Via Sommarive 18, 38123 Trento, Italy*
[b] *Fondazione Bruno Kessler (FBK), Micro Nano Facility (MNF), Via Sommarive 18, 38123 Trento, Italy*
[c] *Department of Engineering, University of Campania "L. Vanvitelli", Via Roma 29, 81031 Aversa, Italy*
[d] *Moresense srl, Filarete Foundation, Viale Ortles 22/4, 20139 Milano, Italy*

ARTICLE INFO

Keywords:
Random antibody
Oriented antibody
XPS
ToF-SIMS
Brucella
Optical and fluorescence detection

ABSTRACT

A successful immunosensor is characterized by a proper antibody immobilization and orientation in order to enhance the antigen recognition. In this work, a thorough characterization of the antibody functionalized gold surface is performed to set up the best conditions to implement in an optical platform for the detection of *Brucella sp*. Two different strategies are evaluated, based on a random immobilization and on an oriented one: a direct antibody immobilization on carboxylic mixed polyethylene (PEG) self-assembled monolayer (SAM) or only carboxylic PEG SAM interface is compared to an oriented immobilization on a layer of protein G on the same PEG SAM interfaces. X-ray Photoelectron Spectroscopy (XPS), Time of Flight Secondary Ion Mass Spectrometry (ToF-SIMS) and contact angle (CA) are used to chemically characterize the gold functionalized surface and ToF-SIMS is also used to confirm the right antibody orientation. Optical characterization is applied to monitor the functionalization steps and fluorescence measurements are used to set up the proper experimental conditions and also to detect *Brucella* bacteria on the surface. Best results are obtained with a 10 ng/μl incubation solution of antibody immobilized, in an oriented way, on a mixed PEG SAM interface.

1. Introduction

A crucial aspect for the realization of good immunosensors is a proper immobilization of the antibody on the sensor surface. There are different strategies for this purpose mainly based on non-covalent interactions (such as electrostatic interaction or entrapment in organic matrices), affinity interactions (using protein A/G or avidin-biotin coupling for instance) or covalent interactions (through amino, thiol or glycol moieties on antibody molecules) [1–8]. The choice of the proper method depends on the sensor surface and there is not a common and general rule. The best protocol has to be set up each time, not only taking into account the surface constrains but also the antigen and the application. General rules can be found in the literature on the best way to immobilize the antibody layer, opportunely choosing the way to bind it to the sensor surface, tailoring the density and controlling the orientation [1,2,4,9], however only few papers report a complete layer characterization and optimization, most merely choosing one recipe and performing the functional tests. There is also the possibility to genetically engineer antibodies (recombinant antibodies) in order to self-assemble on biosensor surfaces achieving a high density and correct orientation to enhance antigen recognition and to increase the sensitivity, specificity, and stability [10]. The building of a functional interface in a well optimized and controlled way is crucial not only to achieve the optimal antigen recognition but also to save reagents, time and to reduce the costs.

One efficient way to immobilize a bioreceptor layer on the sensor surface is through a PEG-SAM [11]: a coupling of the highest accessibility of the bioreceptor for the analyte recognition and a decrease of the non specifc adsorption is obtained. The characteristic "brush" conformation of the PEG-SAMs is in fact known to decrease the non specifc protein adsorption, depending both on the density and the length of the PEG chains [12–15] allowing to identify biomarkers also in complex

* Corresponding authors.
E-mail addresses: l.pasquardini@indiveni.re (L. Pasquardini), luigi.zeni@unicampania.it (L. Zeni).

https://doi.org/10.1016/j.colsurfb.2023.113577
Received 1 May 2023; Received in revised form 8 August 2023; Accepted 30 September 2023
Available online 2 October 2023

biological matrices [16–18]. Among the possible configurations, mixed PEG-SAMs seem to have a better surface control in terms of chemical reactivity [11,19]. Here both mixed and mono short PEG SAMs are evaluated as intermediate layer on gold for the random or oriented immobilization of antibodies.

Brucellosis is an infectious disease caused by bacteria, that can be transferred to humans from animals [20,21]. The most common way to become infected is by eating or drinking unpasteurized/raw dairy products or breathing a bacteria culture, but apart from human disease, brucellosis causes a big economical issue since a certification of positivity implies the slaughtering of all animals in the farm. The recommended initial test for *Brucella* infection identification from the Center for Disease Control and Prevention [22] is based on the agglutination test to detect the presence of anti-brucella antibodies in serum. A value $\geq$ 120 I.U./ml is considered positive to the infection. Other diagnostic assays include mainly microbiological isolation of microorganisms, bacterial identification, and nucleic acid amplification-based methods. Although this is the traditional and the gold standard detection technique, this method is time-consuming, and requires highly skilled technical personnel for handling live cultures that require a laboratory for handling micro-organisms with high biological risk (Biosafety Level 3). Therefore, there is the need to develop sensitive and specific biosensors for the rapid identification of the bacteria in order to contain the infection.

The detection of bacteria using immunosensors is quite widespread [2,3,6,23] and some examples can be found on the detection of *Brucella sp*. [21,24–28]. Most of these examples just reported the selected method, based on random [21,25–28] or oriented antibody [24], without a deep characterization and optimization of the immunosurface. Other biosensors are based on lateral flow assay combined with loop mediated isothermal amplification [29], or on the hybridization on ionic layer-by-layer films coupled to a long-period grating optical fiber [30], on phage-functionalized nanostructures for SERS detection [20] or on aptamer modified QCM chips [31]; moreover, a pathogen enrichment, DNA extraction and hybridization detection through ring resonators [32] or DNA hybridization assays with metal nanoparticles and aggregation in salt-conditions are used [33].

In this work, we design and optimize the interface for the specific recognition of the *Brucella sp*. comparing two different strategies based on random or oriented antibody immobilized on a mixed PEG SAM or a PEG-COOH SAM interface. The random immobilization is obtained by the classical ethyleneimine-carbodiimide coupling chemistry, while the oriented immobilization has an intermediate layer of protein G. The gold derivatization is confirmed using XPS, CA and optical measurements, while ToF-SIMS analysis is mainly used to assess the antibody orientation on the surface. Using fluorescent derivative molecules for antibody and protein G, the protocol is set up to obtain the best experimental conditions. Finally, a functional evaluation of the immuno-layer ability in bacteria recognition is performed, staining the bacteria with a fluorescent dye and performing an automatic counting.

2. Materials and methods

2.1. Materials and reagents

Gold substrates are prepared by depositing 10 nm of titanium on a silicon substrate (100), followed by 100 nm of gold purchased from MicroFabSolution srl (Trento, Italy). M-dPEG®8-Thiol (mPEG) and HS-dPEG™ (12)-COOH (PEG-COOH) for the self-assembled monolayer (SAM) are purchased from Stratech (United Kingdom) and from Iris Biotech GmbH (Marktredwitz, Germany) respectively. 1-ethyl-3-(3-dimethylaminopropyl) carbodiimide hydrochloride (EDC, 22980) and N-hydroxysulfosuccinimide (Sulfo-NHS, 24510) and Pierce recombinant protein G (PtG, 21193) are purchased from Fisher Scientific Italia (Milan, Italy), while the fluorescent derivative Alexafluor488- Protein G (P11065) is purchased from Thermo Scientific (Rockford, IL, USA). Two different antibodies have been used: the monoclonal anti-Brucella antibody produced in mouse (Brucella abortus (Bx88)) is purchased from Santa Cruz Biotechnology, Inc (Heidelberg, Germany) and mouse monoclonal Brucella Abortus Antibody (BrG11) is purchased from Biotechne srl (Milan, Italy). Bovine serum albumin (BSA, A7030), anti-mouse polyvalent immunoglobulins (G,A,M)−FITC, antibody produced in goat (F1010) (IgG FITC) and all powders for buffers are purchased from Sigma-Aldrich s.r.l. (Milan, Italy). Brucella antigenic suspension (BIO-63241), a commercial Brucella solution killed by heat and 4‰ formaldehyde treatment commonly used for agglutination tests, is purchased from Diagnostic International Distribution spa (Milan, Italy). LIVE/DEAD™ BacLight™ Bacterial Viability and Counting Kit (L34856) purchased from Thermo Scientific (Rockford, IL, USA) is used to detect bacteria on functionalized surfaces.

2.2. Substrate functionalization

The gold substrates are first cleaned using an argon plasma for 2 min at 6.8 W to remove organic contaminants. A mixture at 0.2 mM total concentration of an mPEG and PEG-COOH in MilliQ water at room temperature for one hour (spanning different ratios), followed by a washing step in ultrapure water, is used to form the self-assembled monolayer on gold. The activation of carboxylic groups is achieved using a mixture of EDC and sulfo-NHS in 50 mM of MES buffer pH 5.5, with an EDC/sNHS ratio of 40/10 mM for 30 min in orbital shaker. At this point two different strategies are followed, the RANDOM immobilization or the ORIENTED one as reported in Fig. 1. For the RANDOM immobilization, after the carboxylic groups' activation, an antibody solution spanning a range between 1 ÷ 80 ng/μl for one hour in 50 mM of MES buffer pH 5.5 or PBS (10 mM phosphate buffer, 138 mM NaCl, 2.7 mM KCl, pH 7.4) is used. For the ORIENTED strategy instead, a further incubation in a PtG solution (spanning a range between 2 ÷ 100 ng/ μl) in PBS buffer for one hour is performed and then the antibody solution, as previously described, is done. Finally, a passivation step in a solution of 1 % w/v BSA in PBS buffer for 30 min is performed for both strategies.

2.3. Bacteria suspension characterization and detection

The bacterial suspension is characterized staining the bacteria with the Syto®9 component of the Live/Dead kit, according to manufacturer instructions, and using a Thoma cell counter. The fluorescent bacteria are quantified under the microscope, following the protocol instructions. A Leica DMLA fluorescence microscope equipped with a mercury lamp and a fluorescence filter L5 (Leica Microsystems, Germany) is used. The fluorescence is measured with a cooled CCD camera (DFC420C, Leica Microsystems, Germany) and analyzed with the Fiji software [34]. After the bacteria incubation on the surfaces for 5 min, a washing step in PBS is applied for ten times, in order to simulate the real measurement on an SPR platform. The bacteria on the gold surfaces are then stained using 5 μM of Syto®9 for 15 min at dark and then the fluorescence signal is acquired with a 10X magnification objective using the previously described filter and microscope. The quantification is obtained converting the picture in a 8-bit image and setting a threshold as described in Fig. S1. After the threshold selection, bacteria are automatically counted by the software.

2.4. Surface characterization

The chemical characterization of the gold functionalized substrate is performed via CA, XPS and ToF-SIMS. The static contact angle is measured using a home-made system, depositing 2 μl of deionized water droplets on the substrate (at least two drops per sample). The images are acquired with a CMOS camera and analyzed by Drop-Analysis, a plugin of Fiji software [34]. The results are reported as average value and standard deviations.

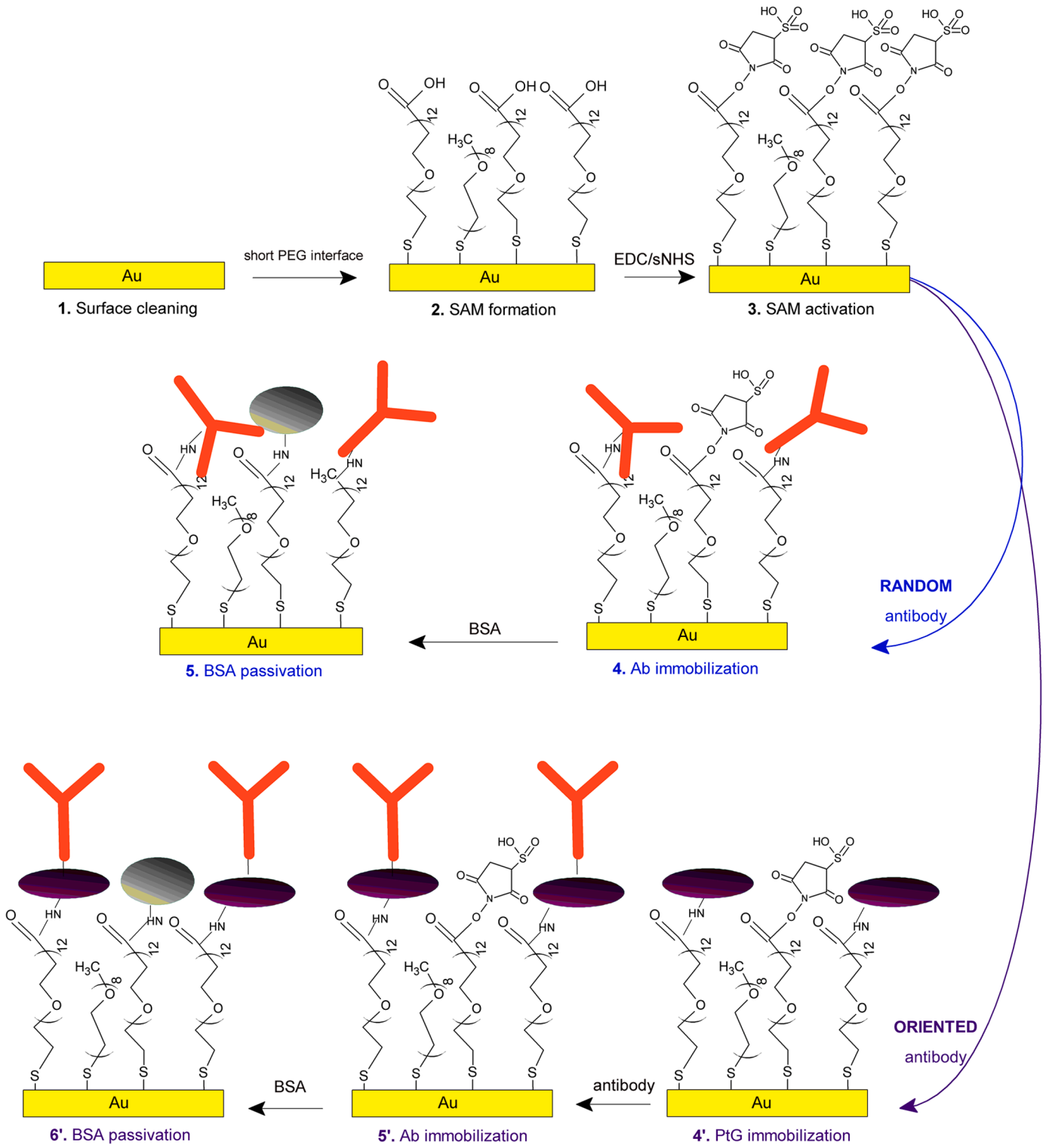

Fig. 1. Scheme of the gold functionalization. After the surface cleaning (1), a short PEG-SAM interface is built (2) and the carboxylic groups are activated through EDC/sNHS chemistry (3). At this point two different strategies are followed: a RANDOM antibody (Ab) immobilization is achieved immediately incubating the activated surface with Ab solution (4) and ending with a BSA passivation (5); while an ORIENTED immobilization is obtained first immobilizing a protein G layer (4') and then the antibody solution (5') and ending with the BSA passivation (6').

XPS analysis is performed using a Kratos Axis Ultra^{DLD} instrument (Kratos Analytical Ltd, England) equipped with a hemispherical analyzer and a monochromatic Al Kα (1486.6 eV) X-ray source, in spectroscopy mode. Photoelectrons were detected at 0° emission angle (sampling depth of about 10 nm [35]) and both survey spectra and O 1 s, C 1 s and Au 4 f core lines are acquired. The relative elemental percentage is obtained by integrating the area under the core lines, applying the Shirley background subtraction, and by correcting for the atomic sensitivity factors through a dedicated software [36].

ToF-SIMS measurements are obtained on a ToF-SIMS IV instrument (ION-TOF GmbH, Germany) equipped with a bismuth liquid metal ion gun (LMIG). SIMS spectra of positive ions are obtained by using Bi_3+

primary ions operated at 25 keV with a pulse width of 19.0 ns and a repetition rate of 10 kHz in the high-current bunched mode. The analysis area (150 × 150 μm^2) is randomly rastered by the primary ions, and the primary ion dose is maintained below static SIMS conditions. The mass resolution (M/ΔM) at $C_7H_7^+$ ($m/z = 91$) is usually more than 7000 and the mass calibration is internally performed by using the H^+, H_2^+, CH_3^+, $C_2H_5^+$, $C_3H_7^+$ and $C_7H_7^+$ peaks; 3 spectra for each sample are collected for statistical reproducibility.

In order to perform a PCA (Principal Component Analysis) of the ToF-SIMS positive secondary ions spectra, a peak list is built by selecting 190 peaks of each spectra. Each peak is normalized to the summation of the selected peaks to eliminate any systematic differences between the spectra, and then mean-centered before the PCA process. With the help of the PCA, a subset of the peaks is created by neglecting all those peaks belonging to the substrate. The remaining peaks (60 peaks) are used to perform PCA analyses on the samples PEG_MIX with RANDOM and ORIENTED antibody.

2.5. Optical characterization

The surface plasmon resonance (SPR) phenomenon can be used to monitor the functionalization processes. More specifically, the bare surface and the surface covered by the receptor layer exhibit different resonance wavelengths when the same bulk solution (typically water or buffer) is present. When the self-assembled bioreceptor is present on the gold surface, the resonance shifts to the right because the refractive index in contact with the plasmonic surface increases. So, the SPR spectra can be applied to monitor, step by step, the functionalization process.

In this work, a miniSPR instrument is used (model Spectra 340 manufactured by Moresense Srl, Milano, in collaboration with University of Campania "L. Vanvitelli"). The experimental setup is based on a spectrometer VIS range 500–730 nm and a white light source 400–780 nm, assembled as reported in Fig. S2. The optical platform is based on SPR plastic optical fiber (POF) chips (model RA1008 manufactured by Moresense Srl, Milano, Italy) built with additive manufacturing technology. The SPR spectra are obtained by a custom Software (named Capture Spectrum Data ver.2.4.8, developed by Moresense Srl, in collaboration with the University of Campania "L. Vanvitelli").

3. Results and discussion

The gold surface is functionalized following the scheme summarized in Fig. 1. After the surface cleaning, a SAM of short PEGs is formed, mixed or only carboxylic PEG; after the carboxylic groups activation through the EDC/sulphoNHS chemistry, the antibody is immobilized directly (RANDOM) or on an orienting protein G layer (ORIENTED) and the surface is finally passivated with BSA solution.

3.1. SAM characterization

SAM formation on the gold surface is assessed by XPS, contact angle measurements and ToF-SIMS analysis. Table 1 reports the value of contact angles measured on the sample while an increasing amount of PEG-COOH is used (last column of Table 1 on the right) and it is clearly evident that increasing the amount of the hydrophilic PEG, a lower value of the contact angle is recorded, as expected. Similar values have been found on silica surfaces using short chains [37] or using PEG-silane molecules [38] and also on gold surfaces [39–41]. In an inversely proportional way, an increase in the oxygen and carbon content is recorded by XPS analysis together with a decrease in the substrate signal (gold). Survey spectra and all significant core levels are reported in the supplementary file (Fig. S3 and Fig. S4). Sulphur is detected in a concentration between 1 % and 2 % maximum on the samples with PEG molecules. A more detailed analysis of the carbon core lines, shows three

Table 1
Chemical characterization determined by XPS and CA on the different samples reported in the first column. XPS data are acquired at 0° take-off angle and standard error does not exceed the 1–2 % of the reported value.

	Sample description	Au (%)	O (%)	C (%)	Carbon components	Contact angle [°]
1	Au	60.7	11.0	28.2	C1 = 16.2 C2 = 8.3 C3 = 3.3	71.9 ± 0.8
2	mPEG	39.6	20.8	39.6	C1 = 1.3 C2 = 37.4 C3 = 0.9	54.7 ± 0.9
3	mPEG_PEG-COOH (0.75:0.25)	36.9	21.6	41.5	C1 = 1.1 C2 = 39.5 C3 = 1.0	44.3 ± 1.9
4	mPEG_PEG-COOH (0.5:0.5)	35.4	22.3	42.2	C1 = 1.1 C2 = 39.7 C3 = 1.4	34.1 ± 1.2
5	mPEG_PEG-COOH (0.25:0.75)	34.8	22.9	42.3	C1 = 1.0 C2 = 39.7 C3 = 1.6	30.7 ± 0.1
6	PEG-COOH	30.0	24.3	45.7	C1 = 1.2 C2 = 42.8 C3 = 1.8	23.1 ± 0.8

peaks attributable to C-C, C-H groups (C1) at approximately 284.6 eV, C-C-O group fingerprint of the PEG molecule (C2) at 286.45 eV [42] and carboxylic group COOH at approximately 289.2 eV (C3) (Fig. S5), in good agreement with the literature [43,44]. Apart from the increase in the PEG fingerprint (C2), an expected increase in the carboxylic group is obtained increasing the PEG-COOH amount in the MIX, even if a small amount is detected also on mPEG SAM only (0.9 %, sample 2 in Table 1). This contribute is clearly not attributable to COOH groups but to other oxidized chemical species, since a TOF-SIMS analysis performed on sample mPEG or PEG-MIX (sample 2 and sample 5 of Table 1) confirmed the absence of carboxylic group on the first sample (see Fig. S6).

3.2. Interface optimization

A fluorescent protein (PtG-AF488) is used to optimize the SAM interface. First, it is used to find the optimal incubation time for the SAM formation, using only mPEG as non-fouling surface. As reported in Fig. S7, one hour is enough to cover the gold surface in an efficient way, since no orientation is necessary in this configuration. Longer incubation times are usually used on SAM of alkanethiol on gold to allow a proper packaging and orientation of the chains; in our system, PEG molecules assume a random orientation since the interaction with water molecules promotes a "brush" conformation [12–15]. Then, a different ratio between the two PEG molecules on EDC/sNHS activated interface is spanned to find the best proportion and achieve the maximum protein immobilization. A mixed PEG SAM in fact is reported to be better in terms of density and accessibility of the functional groups [3]. The obtained results (Fig. S8) suggest that an mPEG_PEG-COOH ratio of 0.25_0.75 (PEG_MIX) is enough to reach the maximum protein immobilization.

On the two selected SAMs (PEG_MIX and PEG-COOH SAM) the PtG concentration is changed to optimize the orienting layer. A range between 2 ÷ 100 ng/μl of PtG is spanned, finding in 50 ng/μl the best concentration (Fig. S9), because, even if higher protein concentration result in higher fluorescence signal, an aspecific adsorption is also observed, especially on PEG-COOH SAM (Fig. S10). Finally, once the SAM interface and the orienting layer have been optimized, we focused on the antibody immobilization, spanning different concentrations and testing two different buffers (MES and PBS): MES buffer is selected because suggested by the manufacturer for the optimal binding on PtG, while PBS is selected because it is the most used buffer for the antibody immobilization. Both RANDOM and ORIENTED immobilization reached the highest antibody immobilization using MES buffer (Fig. 2) on

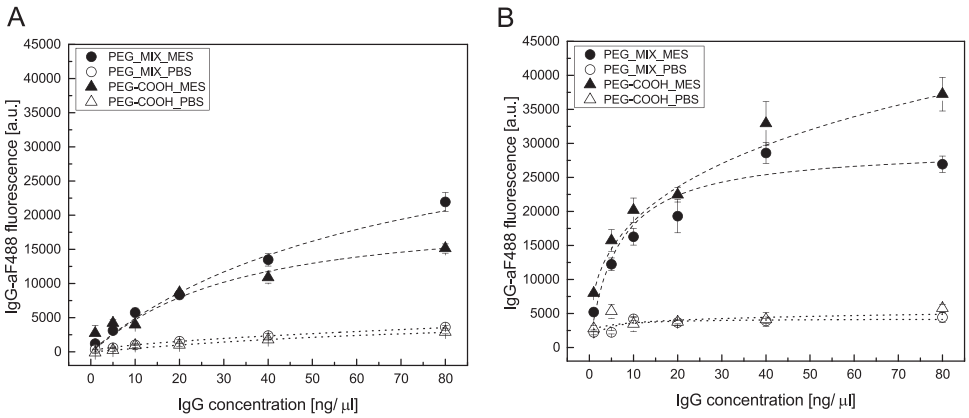

Fig. 2. Incubation of different amount of IgG-AF488 on RANDOM (A) or ORIENTED (B) strategies on PEG_MIX SAM (circles) or PEG-COOH SAM (triangles up) in PBS buffer (white symbols) or MES buffer (dark symbols). Data are reported as mean value of five images and error bars represent the standard deviation. Curves represent the Langmuir fit.

PEG_MIX or PEG-COOH SAM. The use of MES buffer also in the RANDOM immobilization suggests a better orientation also in this case, while a lower pH with respect to the isoelectric point is used [2].

For the ORIENTED strategy a concentration of 40 ng/µl seems to be enough to reach a total coverage of the surface on PEG_MIX SAM interface, while a higher concentration is required for PEG-COOH SAM (Fig. 2B); for the RANDOM strategy a higher concentration is required to saturate the surface in both SAM interfaces (Fig. 2 A).

3.3. Interface characterization

The optimized RANDOM or ORIENTED interface is optically characterized using a miniSPR instrument. Each step of the functionalization process is monitored, recording the spectral shift in the resonance peak. Fig. 3 shows the different behavior between the two interfaces, based on PEG_MIX (A) or on PEG-COOH interface (B): the mixed PEGs SAM (Fig. 3A) is able to better mask the gold surface since BSA incubation does not cause any additional shift, as in the case of PEG-COOH SAM (Fig. 3B). The presence of methoxyPEG in the mixed PEG helps in the biofouling of the surface [12–15]. These results confirmed the behavior observed in fluorescence measurements, where a higher aspecific binding is observed on PEG-COOH SAM (Fig. S10).

The binding of the antibody on the orienting protein G layer is also confirmed by monitoring the variation in the resonance peak position (Fig. 4). The increase in the antibody concentration caused a higher immobilization on the sensor surface and consequently a larger shift is recorded. The Langmuir fit showed saturation at about 40 ng/µl with a correlation coefficient of 0.99, in good agreement with the fluorescence measurements (Fig. 2B).

The antibody orientation is confirmed by ToF-SIMS analysis. The

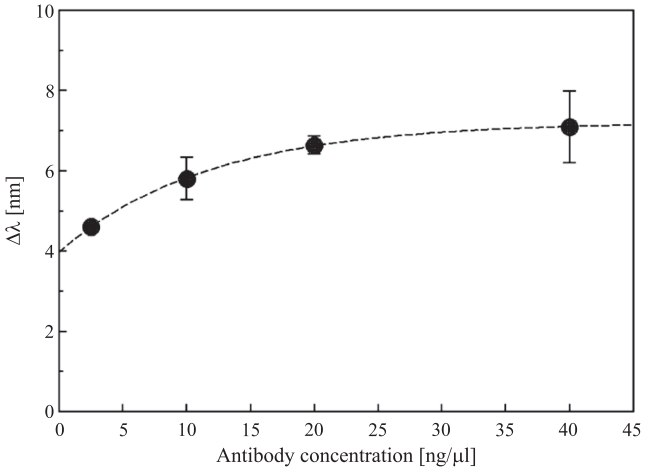

Fig. 4. Resonance shift (Δλ) as function of the antibody concentration. Data are reported as mean values on two independent platforms and error bars represent the standard deviation. Langmuir fit is also reported.

PEG_MIX interface with 40 ng/µl of RANDOM or ORIENTED antibody solution is analyzed to confirm a different orientation of the antibody molecule. Several examples can be found in literature on the application of this technique to identify different aminoacids [45–48]. The two samples resulted well distinguishable as assessed by a Principal Component Analysis (PCA), a multivariate statistical analysis technique, performed on the set of spectra acquired in different areas of the samples

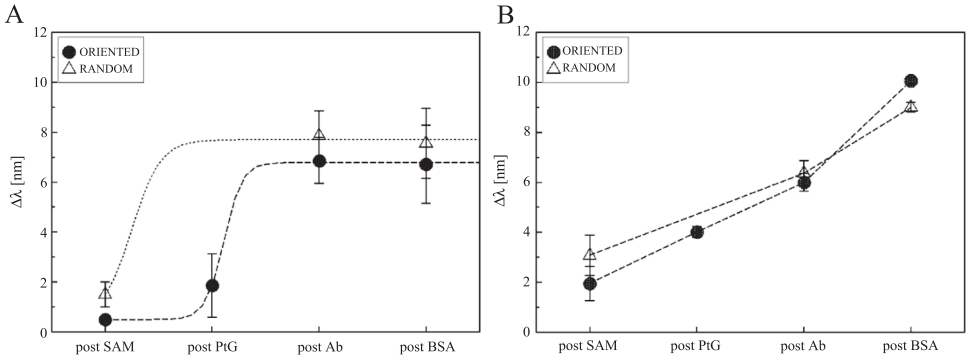

Fig. 3. Resonance shift (Δλ) as a function of the functionalization steps in RANDOM or ORIENTED configuration on platforms with mixed PEG SAM (A) or totally based on PEG-COOH (B). Data are reported as mean values on three independent platforms and the error bars represent the standard deviation.

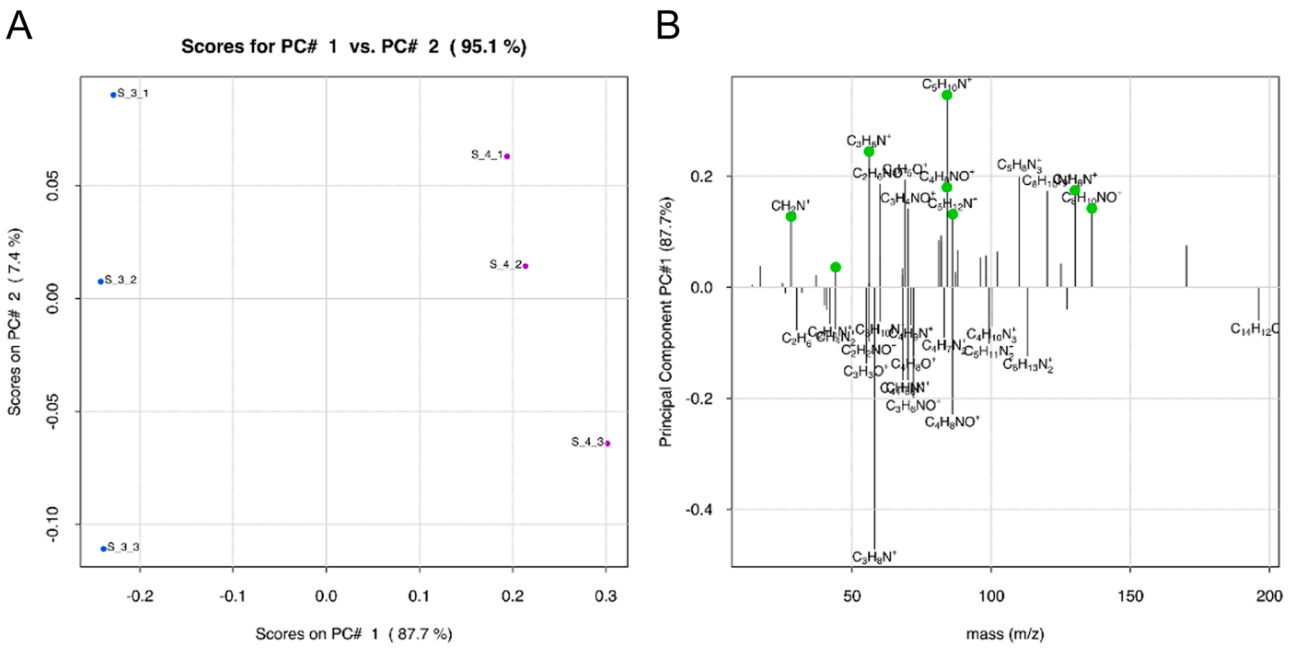

Fig. 5. A) PCA Scores representation of the two set of measurements on RANDOM antibody (S3) and ORIENTED one (S4); B) PCA loadings plot showing the amino acid fragments derived from TOF-SIMS analysis of Fab and Fc fragments immobilized on S3 and S4 surfaces. Fab fragments load in the positive y axis, while amino acid fragments corresponding to the Fc portion load in the negative y axis.

(Fig. 5A): the two datasets resulted separated by more than 95 % of the total variance and along the first principal component, by about 87 %, meaning that the two samples are clearly different. The main amino acids masses are identified in the spectra according to literature [47,48] and can be mainly assigned to the fragment crystallizable (Fc) region or to the antigen binding fragment (Fab) indicative of the possible orientation on the surface: side-on (one Fc and one Fab attached to the surface), tail-on (Fc attached to the surface), head-on (both Fabs attached to the surface) or at-on (all three fragments attached to the surface) [1].

Fig. 5B reports the fragment distribution on S3 (negative part) and S4 (positive part). The fragments mainly attributable to Fab portion are highlighted in green, suggesting that they are present on the S4 sample (the ORIENTED antibody configuration).

3.4. Bacterial recognition

Once the antibody interface is optimized and assessed by chemical-physical techniques, a functional test is applied to definitely find the best conditions for the gold surface functionalization. To this purpose, a bacteria solution of (5.3 ± 1.3) x 10^6 bacteria/ml (as quantify staining bacteria with a fluorescent dye and using a Thoma cell counting, as reported in paragraph 2.3) is applied on the different surfaces for 5 min followed by an extensive washing and staining with fluorescent dye. The two SAM interfaces are analyzed (PEG_MIX and PEG-COOH) with the RANDOM or ORIENTED antibody as a function of the antibody concentration.

Fig. 6 reports the bacteria quantification on the different surfaces. On the PEG_MIX interface it is clearly evident that only in the ORIENTED configuration (Fig. 6B) it is possible to observe a real effect of the antibody that is dependent on the antibody concentration, while in the RANDOM orientation (Fig. 6A) no significative results are obtained with respect to the aspecific adsorption (gray bar). Previously obtained results with fluorescence and optical analysis suggested that a complete antibody coverage of the surface is achieved using a concentration of 40 ng/µl (Fig. 2B and Fig. 4), however a too dense layer is obtained and this can interfere with the recognition of the bacteria [49]. Instead, for the PEG-COOH SAM interface a similar trend is obtained even if the antibody effect seems to be reduced, probably due to a more disordered layer that is unable to guarantee a proper antibody conformation (Fig. 6C and 6D). Two different antibodies are tested without any significant difference (Fig. S11).

4. Conclusions

The correct and efficient immobilization of antibody on the surface is a crucial aspect to build sensitive and specific immunosensors. In this respect, depending on the surface, the proper functionalization method has to be selected according to the final application and performing all the necessary steps to optimize the antibody concentration and orientation. For gold surfaces, a mixed short PEG SAM interface revealed to be the best choice, since the functional groups are properly tuned, and a better accessibility is achieved. Moreover, the mixed PEG SAM contributed to reduce the aspecific adsorption. On this layer, an oriented antibody immobilization through a protein G layer resulted in the best bacteria recognition, once selected the optimal antibody concentration, because a too dense layer interferes with the detection. XPS, ToF-SIMS, CA, optical and fluorescence measurements allowed to set up the optimal conditions for the gold functionalization to be transferred on an SPR optical platform.

CRediT authorship contribution statement

L.P., N.C. and L.Z. conceptualized the work. L.P. performed the experiments and draft the manuscript. R.C. and L.V. conducted the chemical characterization through ToF-SIMS and XPS respectively. C.P, G.D'A., R.P., R.R., A.C., N.C. and L.Z. contributed to the optical device fabrication and optical characterization. All authors interpreted and discussed the results and reviewed the manuscript. N.C. and L.Z. coordinated the work.

Declaration of Competing Interest

The authors declare that they have no known competing financial interests or personal relationships that could have appeared to influence the work reported in this paper.

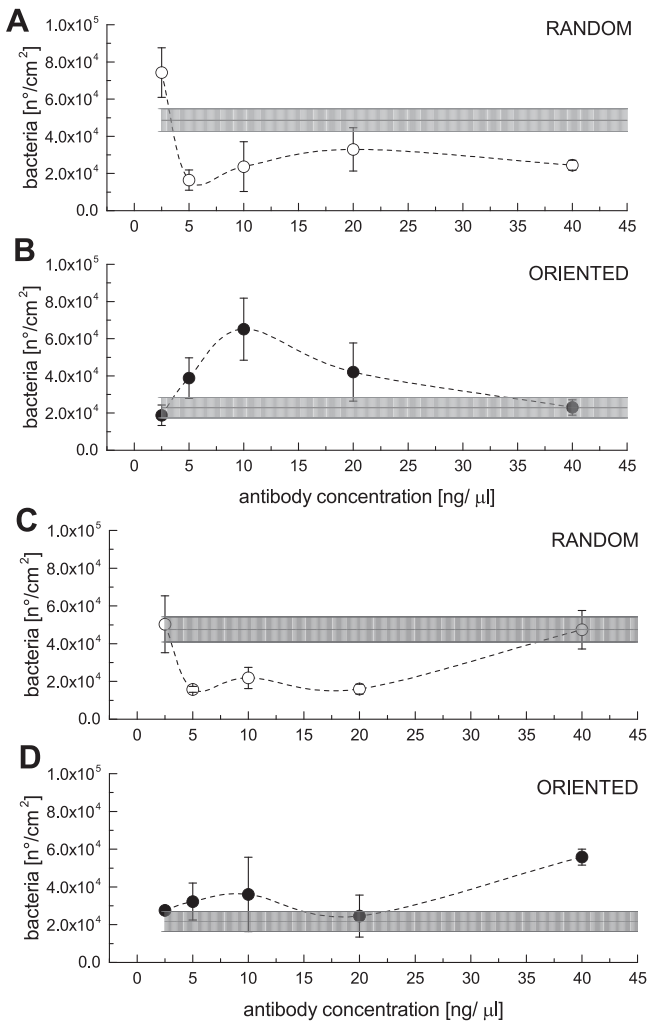

Fig. 6. Fluorescence bacteria recognition on RANDOM or ORIENTED antibody immobilized on PEG_MIX SAM (A,B) or PEG-COOH SAM (C,D) as function of antibody concentration. Data are reported as mean value on five images acquired on the samples and error bars represent the standard deviation. The gray bar represents the aspecific adsorption of bacteria in absence of antibody.

Data availability

Data will be made available on request.

Acknowledgment

This research was funded by ENI-CBC-MED Programme 2014-2020—TRANSDAIRY Project—Funded by EU Grant Contract No. 24/1640.

Appendix A. Supporting information

Supplementary data associated with this article can be found in the online version at doi:10.1016/j.colsurfb.2023.113577.

References

[1] A.K. Trilling, J. Beekwilder, H. Zuilhof, Antibody orientation on biosensor surfaces: a minireview, Analyst 138 (2013) 1619–1627, https://doi.org/10.1039/c2an36787d.

[2] S. Gao, J.M. Guisán, J. Rocha-Martin, Oriented immobilization of antibodies onto sensing platforms - a critical review, Anal. Chim. Acta 1189 (2022), https://doi.org/10.1016/j.aca.2021.338907.

[3] R.A. Taheri, A.H. Rezayan, F. Rahimi, J. Mohammadnejad, M. Kamali, Comparison of antibody immobilization strategies in detection of Vibrio cholerae by surface plasmon resonance, Biointerphases 11 (2016), 041006, https://doi.org/10.1116/1.4971270.

[4] S. Sharma, H. Byrne, R.J. O'Kennedy, Antibodies and antibody-derived analytical biosensors, Essays Biochem. 60 (2016) 9–18, https://doi.org/10.1042/EBC20150002.

[5] J. Guo, S. Noyes, W. Jin, H. Curtis, X. Xu, S. Ghose, Effect of solution condition on the binding behaviors of monoclonal antibody and fusion protein therapeutics in Protein A chromatography, J. Chromatogr. A 1686 (2022), 463652, https://doi.org/10.1016/j.chroma.2022.463652.

[6] Ö. Torun, I. Hakki Boyaci, E. Temür, U. Tamer, Comparison of sensing strategies in SPR biosensor for rapid and sensitive enumeration of bacteria, Biosens. Bioelectron. 37 (2012) 53–60, https://doi.org/10.1016/j.bios.2012.04.034.

[7] V. Vaghi, C. Potrich, L. Lunelli, P. Facci, L. Pasquardini, L. Vanzetti, C. Pederzolli, Bio-functional surfaces for the immunocapture of AGO2-bound microRNAs, Colloids Surf. B Biointerfaces 146 (2016) 746–753, https://doi.org/10.1016/j.colsurfb.2016.06.059.

[8] L. Pasquardini, N. Cennamo, G. Malleo, L. Vanzetti, L. Zeni, D. Bonamini, R. Salvia, C. Bassi, A.M. Bossi, A surface plasmon resonance plastic optical fiber biosensor for the detection of pancreatic amylase in surgically-placed drain effluent, Sensors 21 (2021) 1–15, https://doi.org/10.3390/s21103443.

[9] M.B. Young, B.K. Oh, W. Lee, H.L. Won, J.W. Choi, Study on orientation of immunoglobulin G on protein G layer, Biosens. Bioelectron. 21 (2005) 103–110, https://doi.org/10.1016/j.bios.2004.09.003.

[10] X. Zeng, Z. Shen, R. Mernaugh, Recombinant antibodies and their use in biosensors, Anal. Bioanal. Chem. 402 (2012) 3027–3038, https://doi.org/10.1007/s00216-011-5569-z.

[11] J.P. Folkers, P.E. Laibinis, G.M. Whitesides, J. Deutch, Phase behavior of two-component self-assembled monolayers of alkanethiolates on gold, J. Phys. Chem. 98 (1994) 563–571, https://doi.org/10.1021/j100053a035.

[12] A.R. Lokanathan, S. Zhang, V.R. Regina, M.A. Cole, R. Ogaki, M. Dong, F. Besenbacher, R.L. Meyer, P. Kingshott, Mixed poly (ethylene glycol) and oligo (ethylene glycol) layers on gold as nonfouling surfaces created by backfilling, Biointerphases 6 (2011) 180–188, https://doi.org/10.1116/1.3647506.

[13] C. Zhang, J. Lu, Y. Hou, W. Xiong, K. Sheng, H. Lu, Investigation on the linker length of synthetic zwitterionic polypeptides for improved nonfouling surfaces, ACS Appl. Mater. Interfaces 10 (2018) 17463–17470, https://doi.org/10.1021/acsami.8b02854.

[14] A. Rafati, A.G. Shard, D.G. Castner, Multitechnique characterization of oligo (ethylene glycol) functionalized gold nanoparticles, Biointerphases 11 (2016), https://doi.org/10.1116/1.4967216.

[15] K. Zhao, M. Li, P. Zhang, J. Cui, Sticktight-inspired PEGylation for low-fouling coatings, Chem. Commun. 58 (2022) 13735–13738, https://doi.org/10.1039/d2cc04938d.

[16] H. Vaisocherová, E. Brynda, J. Homola, Functionalizable low-fouling coatings for label-free biosensing in complex biological media: advances and applications, Anal. Bioanal. Chem. 407 (2015) 3927–3953, https://doi.org/10.1007/s00216-015-8606-5.

[17] R. D'Agata, N. Bellassai, M.C. Giuffrida, A.M. Aura, C. Petri, P. Kögler, G. Vecchio, U. Jonas, G. Spoto, A new ultralow fouling surface for the analysis of human plasma samples with surface plasmon resonance, Talanta 221 (2021), https://doi.org/10.1016/j.talanta.2020.121483.

[18] X. Yang, P. Chen, X. Zhang, H. Zhou, Z. Song, W. Yang, X. Luo, An electrochemical biosensor for HER2 detection in complex biological media based on two antifouling materials of designed recognizing peptide and PEG, Anal. Chim. Acta 1252 (2023), 341075, https://doi.org/10.1016/j.aca.2023.341075.

[19] S.V. Atre, B. Liedberg, D.L. Allara, Chain length dependence of the structuee and wetting properties in binary composition monolayers of OH- and CH3-terminated alkanethiolates on gold, Langmuir 11 (1995) 3882–3893, https://doi.org/10.1021/la00010a045.

[20] M. Rippa, R. Castagna, D. Sagnelli, A. Vestri, G. Borriello, G. Fusco, J. Zhou, L. Petti, SERS biosensor based on engineered 2D-aperiodic nanostructure for in-situ detection of viable brucella bacterium in complex matrix, Nanomaterials 11 (2021) 7–9, https://doi.org/10.3390/nano11040886.

[21] R. Wahab, S.T. Khan, J. Ahmad, J. Musarrat, A.A. Al-Khedhairy, Functionalization of anti-Brucella antibody on ZnO-NPs and their deposition on aluminum sheet towards developing a sensor for the detection of Brucella, Vacuum 146 (2017) 592–598, https://doi.org/10.1016/j.vacuum.2017.01.019.

[22] CDC, No Title, (n.d.). ⟨https://www.cdc.gov/brucellosis/clinicians/serology.html⟩ (accessed July 29, 2023).

[23] B. Péter, E. Farkas, S. Kurunczi, Z. Szittner, S. Bősze, I. Szekacs, R. Horvath, J. J. Ramsden, Review of label-free monitoring of bacteria: from challenging practical applications to basic research perspectives, Biosensors 12 (2022), https://doi.org/10.3390/bios12040188.

[24] S.L. Baltierra-Uribe, J.J. Chanona-Pérez, J.V. Méndez-Méndez, M. de, J. Perea-Flores, A.C. Sánchez-Chávez, B.E. García-Pérez, M.C. Moreno-Lafont, R. López-Santiago, Detection of Brucella abortus by a platform functionalized with protein A and specific antibodies IgG, Microsc. Res. Tech. 82 (2019) 586–595, https://doi.org/10.1002/jemt.23206.

[25] A. Shams, B. Rahimian Zarif, Designing an immunosensor for detection of Brucella abortus based on coloured silica nanoparticles, Artif. Cells Nanomed. Biotechnol. 47 (2019) 2562–2568, https://doi.org/10.1080/21691401.2019.1626403.

[26] H. Wu, Y. Zuo, C. Cui, W. Yang, H. Ma, X. Wang, Rapid quantitative detection of Brucella melitensis by a label-free impedance immunosensor based on a gold

nanoparticle-modified screen-printed carbon electrode, Sensors (Switzerland) 13 (2013) 8551–8563, https://doi.org/10.3390/s130708551.
[27] H. Taheri, B. Amini, M. Kamali, M. Asadi, E. Naderlou, Functionalization of anti-Brucella antibody based on SNP and MNP nanoparticles for visual and spectrophotometric detection of Brucella, Spectrochim. Acta - Part A Mol. Biomol. Spectrosc. 229 (2020), 117891, https://doi.org/10.1016/j.saa.2019.117891.
[28] H. Chen, H. Liu, C. Cui, X. Zhang, W. Yang, Y. Zuo, Highly sensitive detection of Brucella in milk by cysteamine functionalized nanogold/4-Mercaptobenzoic acid electrochemical biosensor, J. Food Meas. Charact. 16 (2022), https://doi.org/10.1007/s11694-022-01428-9.
[29] S. Li, Y. Liu, Y. Wang, H. Chen, C. Liu, Y. Wang, Lateral flow biosensor combined with loop-mediated isothermal amplification for simple, rapid, sensitive, and reliable detection of Brucella spp, Infect. Drug Resist. 12 (2019) 2343–2353, https://doi.org/10.2147/IDR.S211644.
[30] K. McCutcheon, A.B. Bandara, Z. Zuo, J.R. Heflin, T.J. Inzana, The application of a nanomaterial optical fiber biosensor assay for identification of Brucella nomenspecies, Biosensors 9 (2019) 1–14, https://doi.org/10.3390/bios9020064.
[31] G. Bayramoglu, V.C. Ozalp, M. Oztekin, M.Y. Arica, Rapid and label-free detection of Brucella melitensis in milk and milk products using an aptasensor, Talanta 200 (2019) 263–271, https://doi.org/10.1016/j.talanta.2019.03.048.
[32] F. Zhao, B. Koo, H. Liu, C. Eun Jin, Y. Shin, A single-tube approach for in vitro diagnostics using diatomaceous earth and optical sensor, Biosens. Bioelectron. 99 (2018) 443–449, https://doi.org/10.1016/j.bios.2017.08.027.
[33] D. Pal, N. Boby, S. Kumar, G. Kaur, S.A. Ali, J. Reboud, S. Shrivastava, P.K. Gupta, J.M. Cooper, P. Chaudhuri, Visual detection of Brucella in bovine biological samples using DNA-activated gold nanoparticles, PLoS One 12 (2017), https://doi.org/10.1371/journal.pone.0180919.
[34] C.A. Schneider, W.S. Rasband, K.W. Eliceiri, NIH Image to ImageJ: 25 years of image analysis, Nat. Methods 9 (2012) 671–675, https://doi.org/10.1038/nmeth.2089.
[35] Z. Li, W. Han, D. Kozodaev, J.C.M. Brokken-Zijp, G. de With, P.C. Thüne, Surface properties of poly(dimethylsiloxane)-based inorganic/organic hybrid materials, Polymer (Guildf) 47 (2006) 1150–1158, https://doi.org/10.1016/j.polymer.2005.12.057.
[36] G. Speranza, R. Canteri, RxpsG a new open project for photoelectron and electron spectroscopy data processing, SoftwareX 10 (2019), 100282, https://doi.org/10.1016/j.softx.2019.100282.
[37] A. Hasan, G. Waibhaw, L.M. Pandey, Conformational and organizational insights into serum proteins during competitive adsorption on self-assembled monolayers, Langmuir 34 (2018) 8178–8194, https://doi.org/10.1021/acs.langmuir.8b01110.
[38] S. Jo, K. Park, Surface modification using silanated poly(ethylene glycol)s, Biomaterials 21 (2000) 605–616, https://doi.org/10.1016/S0142-9612(99)00224-0.
[39] J.A. Jones, L.A. Qin, H. Meyerson, I.K. Kwon, T. Matsuda, J.M. Anderson, Instability of self-assembled monolayers as a model material system for macrophage/FBGC cellular behavior, J. Biomed. Mater. Res. Part A 86A (2008) 261–268, https://doi.org/10.1002/jbm.a.31660.
[40] S. Yao, X. Liu, J. He, X. Wang, Y. Wang, F.Z. Cui, Ordered self-assembled monolayers terminated with different chemical functional groups direct neural stem cell linage behaviours, Biomed. Mater. 11 (2015) 14107, https://doi.org/10.1088/1748-6041/11/1/014107.
[41] T. Satomi, Y. Nagasaki, H. Kobayashi, T. Tateishi, K. Kataoka, H. Otsuka, Physicochemical characterization of densely packed poly(ethylene glycol) layer for minimizing nonspecific protein adsorption, J. Nanosci. Nanotechnol. 7 (2007) 2394–2399, https://doi.org/10.1166/jnn.2007.695.
[42] G. Beamson, D. Briggs, High resolution XPS of organic polymers: the Scienta ESCA300 database, J. Wiley & Sons Chichester, Chichester SE, 1992 https://doi.org/ LK - https://worldcat.org/title/468388173.
[43] G. Liu, S. Wang, J. Liu, D. Song, An electrochemical immunosensor based on chemical assembly of vertically aligned carbon nanotubes on carbon substrates for direct detection of the pesticide endosulfan in environmental water, Anal. Chem. 84 (2012) 3921–3928, https://doi.org/10.1021/ac202754p.
[44] A. Al-Ani, A. Boden, M. Al Kobaisi, H. Pingle, P.Y. Wang, P. Kingshott, The influence of PEG-thiol derivatives on controlling cellular and bacterial interactions with gold surfaces, Appl. Surf. Sci. 462 (2018) 980–990, https://doi.org/10.1016/j.apsusc.2018.08.136.
[45] I.H. Cho, J.W. Park, T.G. Lee, H. Lee, S.H. Paek, Biophysical characterization of the molecular orientation of an antibody-immobilized layer using secondary ion mass spectrometry, Analyst 136 (2011) 1412–1419, https://doi.org/10.1039/c0an00672f.
[46] E.T. Harrison, Y.-C. Wang, L. Carter, D.G. Castner, Characterizing protein G B1 orientation and its effect on immunoglobulin G antibody binding using XPS, ToF-SIMS, and quartz crystal microbalance with dissipation monitoring, Biointerphases 15 (2020), 021002, https://doi.org/10.1116/1.5142560.
[47] V. Lebec, S. Boujday, C. Poleunis, C.M. Pradier, A. Delcorte, Time-of-flight secondary ion mass spectrometry investigation of the orientation of adsorbed antibodies on sams correlated to biorecognition tests, J. Phys. Chem. C. 118 (2014) 2085–2092, https://doi.org/10.1021/jp410845g.
[48] F. Liu, M. Dubey, H. Takahashi, D.G. Castner, D.W. Grainger, Immobilized antibody orientation analysis using secondary ion mass spectrometry and fluorescence imaging of affinity-generated patterns, Anal. Chem. 82 (2010) 2947–2958, https://doi.org/10.1021/ac902964q.
[49] L. Sola, L. Abdel Mallak, F. Damin, A. Mussida, D. Brambilla, M. Chiari, Optimization of functional group concentration of N, N-dimethylacrylamide-based polymeric coatings and probe immobilization for DNA and protein microarray applications, Micromachines 14 (2023) 302, https://doi.org/10.3390/mi14020302.